Available online at www.sciencedirect.com

ScienceDirect

IFAC PapersOnLine 51-24 (2018) 824–830

Adaptive dynamic control allocation for over-actuated dynamic positioning system based on backstepping method in case of thruster faults

Anna Witkowska*, Roman Śmierzchalski**

* *Gdansk University of Technology, Department of Electrical and Control Engineering, Narutowicza 11/12, 80-233 Gdansk, Poland (Tel: (+48) 58 347 12 70; email:anna.witkowska@pg.edu.pl).*

***Gdansk University of Technology, Department of Electrical and Control Engineering, Narutowicza 11/12, 80-233 Gdansk, Poland, (email:roman.smierzchalski@pg.edu.pl)*

Abstract: The objective of the research considered in this paper is dynamic positioning of a nonlinear over-actuated marine vessel in the presence of limited information about thruster forces. First, the adaptive backstepping method is used to estimate the input matrix which will compensate partial loss of actuator effectiveness in the presence of actuator dynamics. Then, the adaptive commanded virtual forces and moment are allocated into individual thrusters by employing the control allocation algorithm to compensate total faults. The effectiveness of the proposed control scheme is demonstrated by simulations involving a redundant set of actuators, when actuators lose partially their efficiency or failed.

Keywords: thruster faults, backstepping, control allocation, adaptive control, dynamic positioning.

1. INTRODUCTION

Ship motion control at low speed makes use of the dynamic positioning system (DPS) the main goal of which is to maintain ship position and heading in the presence of environmental disturbances. This task is performed through the control in three degrees of freedom, by using thrusters and propellers which can generate forces and moment in different directions of motion. The multi-layer dynamic positioning (DP) control structure comprises two main control loops. The first of them is the open loop with the wind feedforward block, in which the coupling signal is generated by the wind disturbance model. The second loop is the main closed control loop, in which the commanded values of ship position and orientation (given by the heading) are compared with those estimated from state observation and wave filtering. The closed control loop cooperates with the set of controllers, which are: the position and heading DP controller (high level controller), the control allocation (CA) system (optimisation based process), and the actuator controller (low level controller). The high-level controller controls the ship motion independently in three degrees of freedom. It calculates the generalized vector of commanded longitudinal force, transverse force, and moment to compensate deflections from the desired values, according to the assumed error of control. The control algorithm generates the set signals for the control allocation system that calculates the law of dividing the commanded forces and moment into particular commanded settings of actuators. The actuator controller determines the actuator settings which fulfil the actuator dynamics, taking into account physical constraints of actuators' demands. The set of controllers can be analysed separately based on the separation principle, and the interconnection between them, see Loria et al. (2000).

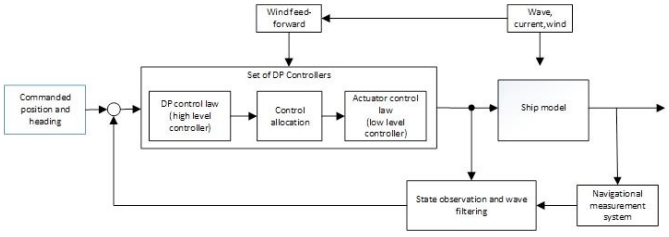

Figure 1. Simplified diagram of ship dynamic positioning control system.

A survey of selected major research works and technology advances in the field of dynamic positioning (DP) controller design was summarized by Sorensen, (2011). In modern DP vessels, the total number of control inputs exceeds the total number of controlled degrees of freedom, so the type of over-actuated control takes place. The exact number of control inputs may differ depending on tasks performed by the DP ship, DP Classes, ship size and economic conditions. The CA system takes into account physical constraints of rudder and propulsion operation, (e.g. input saturation and rate constraints), steering and propulsion efficiency, configuration, as well as constraints resulting from current amount of electric and mechanical power available on the ship. A solution is searched which will allow to obtain minimal energy losses and wear of actuators when executing the basic goal of control, which is precise ship positioning. A detailed overview of the existing control allocation methods can be found in (Johansen and Fossen, 2013).

The control allocation problem is mostly viewed as a static or quasi-dynamic optimization problem that is solved

10.1016/j.ifacol.2018.09.670

independently of the dynamic control problem considering non-adaptive linear effector models and neglecting the actuator dynamics. The simplest of the presented solutions consist in calculating a pseudo-inverse matrix and the use of classical optimisation methods, such as the Lagrange method or the least square method to minimise the activity of the actuators. More complicated solutions consist of numerous optimisation methods to take into account constraints connected with saturation of actuators: penalty function, direct allocation (DA) method, redistributed pseudo-inverse (RPI) method (Oppenheimer et al. 2006), cascading generalized inverse (CGI) (Lindegaard and Fossen, 2003). The linear actuator dynamics is considered by using model predictive control allocation (MPCA) (Oppenheimer et al. 2004). However, control allocation (CA) algorithms do not usually provide robustness to uncertainties in the control effectiveness matrix, which is of basic importance for practical applications especially during actuator failure. The uncertainties result from actuator configuration and thrust losses, which depend on environmental conditions, water density, ship velocity and actuator faults. In the case of actuator fault information, the control effectiveness matrix is usually estimated by the Fault Detection and Diagnosis (FDD) systems, which are strongly committed to the fault-tolerant control strategy. Fault-tolerant (FT) approaches addressed to DP control system have been recently proposed by Benetazzo et al. (2015), Lin and Du (2016), Zhang and Yang (2017), Su et al. (2017). The disadvantage of these approaches is that they require the fault detection and isolation mechanism to be included directly in the control law formulation. Another way to reduce the effect of thrust losses is using adaptive dynamic control allocation strategy. This approach to designing DP systems was presented in the literature by Tjønnås and Johansen (2005, 2007). In those papers, instead of optimizing the control allocation at each time instant, a dynamic approach was considered by constructing update-laws that represent asymptotically optimal allocation search and adaptation formulated based on the Lagrangian function and the Lyapunov theory.

This paper presents a design of adaptive dynamic control allocation for an over-actuated dynamic positioning vessel based on the adaptive vectorial backstepping (Krsti'c et al. 1995) and sequential quadratic programming (Johansen and Fossen, 2013) as an alternative formulation to accommodate to thrust uncertainties. In our paper the control allocation problem is considered with respect to uncertainty in the control effectiveness matrix as a function of operating point variables. First, the high-level motion control based backstepping algorithm is developed to update the commanded forces and moment in the presence of the unknown: control effectiveness matrix, ship dynamics model parameters, and environmental disturbances. Furthermore, the control allocation based sequential quadratic programming was used for actuator-force mapping, to divide the updated commanded forces and moment into particular commanded settings of actuators, and to compensate total actuator faults. The relevant element of this structure is a detailed algorithm to estimate the control effectiveness matrix for the proposed DP control system without a priori knowledge of vessel's model parameters and slowly varying disturbances. Additionally, the linear time-varying actuator dynamics is taken directly into control law formulation.

2. MATHEMATICAL SHIP MODEL

The multivariable nonlinear mathematical model of DP marine vessel in 3 DOF is formulated in the state-space representation (1)-(3) (Fossen, 2011):

$$\dot{\boldsymbol{\eta}} = \mathbf{J}(\boldsymbol{\eta})\mathbf{v} \tag{1}$$

$$\mathbf{M}\dot{\mathbf{v}} = \boldsymbol{\tau} + \boldsymbol{\varphi}_1^T(\boldsymbol{\eta}, \mathbf{v})\boldsymbol{\theta}_1 \tag{2}$$

$$\dot{\mathbf{u}} = \mathbf{T}^{-1}(\mathbf{u}_c - \mathbf{u}) \tag{3}$$

where:

$\mathbf{u}_c$ represents controls and $\boldsymbol{\eta}, \mathbf{v}, \mathbf{u}$ represent states.

$\boldsymbol{\varphi}_1^T(\boldsymbol{\eta}, \mathbf{v})\boldsymbol{\theta}_1 = -\mathbf{D}\mathbf{v} + \mathbf{J}(\boldsymbol{\eta})^T\mathbf{b} \in \mathrm{R}^{3\times 1}$

$\boldsymbol{\theta}_1 = [X_u, Y_v, Y_r, N_v, N_r, b_1, b_2, b_3]^T \in \mathrm{R}^{8\times 1}$

$$\boldsymbol{\varphi}_1^T(\boldsymbol{\eta}, \mathbf{v}) = \begin{bmatrix} u & 0 & 0 & 0 & 0 & cos\psi & sin\psi & 0 \\ 0 & v & r & 0 & 0 & -sin\psi & cos\psi & 0 \\ 0 & 0 & 0 & v & r & 0 & 0 & 1 \end{bmatrix} \in \mathrm{R}^{3\times 8}$$

Equations (1)-(3) describe, ship kinematics (1), dynamics (2), and actuator dynamics (3). The state vector $\boldsymbol{\eta} = [x, y, \psi]^{\mathrm{T}} \in \mathrm{R}^3$ consists of ship's position (x,y) and heading $\psi \in [0, 2\pi]$ in the earth-fixed frame, the state vector $\mathbf{v} = [u, v, r]^{\mathrm{T}} \in \mathrm{R}^3$ denotes the ship's forward, lateral and angular velocity in the body-fixed frame, and the vector $\boldsymbol{\tau} = [\tau_x, \tau_y, \tau_n]^{\mathrm{T}} \in \mathrm{R}^3$ represents generalized forces and moment coming from the thrusters and propulsion devices (actuators) in the body-fixed frame. The component $\mathbf{J}(\boldsymbol{\eta})^T\mathbf{b} = \boldsymbol{\tau}_{env} \in \mathrm{R}^3$ describes unmodelled dynamics and slowly varying environmental disturbances which are generated by wind, wave loads, and can be counteracted by the control inputs. The vector $\mathbf{u} \in \mathrm{R}^{\mathrm{r}\times 1}$ represents actual r ($\mathrm{r} \geq 3$) actuator states and $\mathbf{u}_c \in \mathrm{R}^{\mathrm{r}\times 1}$ is the control input vector to the plant. Other terms represent: $\mathbf{b} = [b_1, b_2, b_3]^T \in \mathrm{R}^{3\times 1}$ – the bias term modelled by 1-st order Markov process; $\mathbf{J} \in \mathrm{R}^{3\times 3}$ – the state-dependent transformation matrix from the vessel-fixed to the earth-fixed frame; $\mathbf{D} \in \mathrm{R}^{3\times 3}$ - the linear matrix related to hydrodynamic damping forces and moments X_u, Y_v, N_v, Y_r, N_r, acting on the vessel during ship movement on the water; $\mathbf{M} \in \mathrm{R}^{3\times 3}$ – the system inertia matrix, which includes vessel's rigid-body and hydrodynamic added inertia; $\mathbf{T} \in \mathrm{R}^{\mathrm{r}\times\mathrm{r}}$ is the diagonal matrix of actuator's time constants.

The relation between the thruster forces and moment $\boldsymbol{\tau}$ acting on the vessel, and the actuator state vector $\mathbf{u}$ is included in the thruster model (force generation model):

$$\boldsymbol{\tau} = \boldsymbol{\theta}_2 \mathbf{I}\mathbf{u} \tag{4}$$

where

$\boldsymbol{\theta}_2 = \mathbf{B}(\boldsymbol{\alpha})\mathbf{K}(U) \in \mathrm{R}^{3\times\mathrm{r}}$,

$\mathbf{K}(U) = diag([k_1\ k_2\ k_3 \ldots k_r]) \in \mathrm{R}^{\mathrm{r}\times\mathrm{r}} > 0$ – control effectiveness matrix,

$\mathbf{B}(\boldsymbol{\alpha}) \in \mathrm{R}^{3\times\mathrm{r}}$ - the actuator configuration matrix

Matrix $\mathbf{B}(\boldsymbol{\alpha}) \in \mathrm{R}^{3\times\mathrm{r}}$ depends on the locations of actuators and the vector of thrust angles $\boldsymbol{\alpha}$ (in the case of rotatable thrusters). Matrix $\mathbf{I} = diag(e_1, \ldots, e_{\mathrm{r}})$ is introduced to contain the

information about the actuator total fault. The case $e_i = 1$ for the *i*-th actuator indicates the total fault-free case, while $e_i = 0$ indicates that total loss of effectiveness has occurred on the *i*-th actuator (Su et al. 2017).

An aspect of DP ship control, the uncertainties in force generation model (4) result from thrust losses. It has the form of partial thrust loss, which depends on ship's velocity, density of water, propeller's diameter and revolutions, disturbances, types of actuators, and thrust loss resulting from failure of one of propellers. Depending on the scale of failure, distinction can be made between partial faults and total faults. The term partial fault means the state in which the ship retains manoeuvring ability, despite the propeller failure. This leads to changes of **K** matrix parameters in the force generation model. In that case the proposed adaptation system adapts to the recorded changes. Deviation from the set limiting values of selected parameters, or changes in selected operating conditions are signaled by the alarm system. On the other hand, when the critical state, i.e. the total fault is reached, the safety system disconnects the faulty propeller. The information on this state is passed to the control system, for instance via FDD systems. In the proposed control structure, the information that total loss of effectiveness has occurred on the actuators is stored in matrix **I**.

The following assumption can be made when designing the control law:

Assumption 1:

1. The matrices **D, K** and **B** are assumed to be unknown, so the vector $\boldsymbol{\theta}_1$ and the matrix $\boldsymbol{\theta}_2$ contain unknown elements.
2. All states are available for feedback and bounded. It is assumed that the vessel position and heading are measured and filtered while the unmeasured velocity vector is estimated, and their estimated values converge/are near to the real ones.
3. The position reference trajectories $\boldsymbol{\eta}_\mathrm{d}$ and their first and second-order derivatives $\dot{\boldsymbol{\eta}}_\mathrm{d}$, $\ddot{\boldsymbol{\eta}}_\mathrm{d}$ are smooth and bounded.
4. Slowly varying environmental disturbances **b** are unknown.
5. The information about total faults of actuators is known. The matrix **I** is known.

3. DP CONROLLER AND CONTROL ALLOCATION

3.1 Backstepping controller

Following the backstepping methodology, the error vectors $\mathbf{z}_1(t) \in \mathrm{R}^{3\times1}$, $\mathbf{z}_2(t) \in \mathrm{R}^{3\times1}$, and $\mathbf{z}_3(t) \in \mathrm{R}^{3\times1}$ are defined in the body-fixed coordinate system (5)-(7) for kinematic, dynamic and actuator subsystems, respectively.

$$\mathbf{z}_1 = \mathbf{J}(\boldsymbol{\eta})^T(\boldsymbol{\eta} - \boldsymbol{\eta}_\mathrm{d}) \quad (5)$$

$$\mathbf{z}_2 = \mathbf{v} - \boldsymbol{\alpha}_1 \quad (6)$$

$$\mathbf{z}_3 = \widehat{\boldsymbol{\theta}}_2\mathbf{I}\mathbf{u} - \boldsymbol{\alpha}_2 \quad (7)$$

where $\widehat{\boldsymbol{\theta}}_2$ denotes the estimate of $\boldsymbol{\theta}_2$, both satisfying **Assumption 1.5.**

The time derivative of $\mathbf{z}_1$ is calculated based on (5), (1) and using **Assumption 1.2-1.3**

$$\begin{aligned}\dot{\mathbf{z}}_1 &= \tfrac{d\,\mathbf{J}(\boldsymbol{\eta})^T}{dt}(\boldsymbol{\eta} - \boldsymbol{\eta}_d) + \mathbf{J}(\boldsymbol{\eta})^T(\dot{\boldsymbol{\eta}} - \dot{\boldsymbol{\eta}}_d)\\ &= -r\mathbf{S}\mathbf{z}_1 + \mathbf{v} - \mathbf{J}(\boldsymbol{\eta})^T\dot{\boldsymbol{\eta}}_d\end{aligned} \quad (8)$$

Consequently substituting (6) to (8) yields

$$\dot{\mathbf{z}}_1 = -r\mathbf{S}\mathbf{z}_1 + \mathbf{z}_2 + \boldsymbol{\alpha}_1 - \mathbf{J}(\boldsymbol{\eta})^T\dot{\boldsymbol{\eta}}_d \quad (9)$$

In the light of (6) and (2) the time derivative of $\mathbf{z}_2$ is in the form

$$\dot{\mathbf{z}}_2 = \dot{\mathbf{v}} - \dot{\boldsymbol{\alpha}}_1 = \mathbf{M}^{-1}\left(\boldsymbol{\theta}_2\mathbf{I}\mathbf{u} + \boldsymbol{\varphi}_1^T(\boldsymbol{\eta},\mathbf{v})\boldsymbol{\theta}_1 - \mathbf{M}\dot{\boldsymbol{\alpha}}_1\right). \quad (10)$$

From (7) and according to **Assumption 1.5,** we get

$$\mathbf{I}\mathbf{u} = \widehat{\boldsymbol{\theta}}_2^{+}(\mathbf{z}_3 + \boldsymbol{\alpha}_2) \quad (11)$$

The natural way of finding the adaptive control law for $\boldsymbol{\theta}_i$ consist in using the principle certainty equivalence, where the uncertainties $\boldsymbol{\theta}_i$ are replaced in (10) by the sum $\widehat{\boldsymbol{\theta}}_i + \widetilde{\boldsymbol{\theta}}_i$ of estimates and estimation errors. Then, substituting (11) into (10) yields

$$\begin{aligned}\dot{\mathbf{z}}_2 = \mathbf{M}^{-1}\left(\mathbf{z}_3 + \boldsymbol{\alpha}_2 + \boldsymbol{\varphi}_1^T(\boldsymbol{\eta},\mathbf{v})\widehat{\boldsymbol{\theta}}_1\right) +\\ \mathbf{M}^{-1}(\widetilde{\boldsymbol{\theta}}_2\mathbf{I}\mathbf{u} + \boldsymbol{\varphi}_1^T(\boldsymbol{\eta},\mathbf{v})\widetilde{\boldsymbol{\theta}}_1) - \dot{\boldsymbol{\alpha}}_1\end{aligned} \quad (12)$$

The time derivative of $\mathbf{z}_3$ is calculated based on (7) and (3)-(4)

$$\begin{aligned}\dot{\mathbf{z}_3} &= \widehat{\boldsymbol{\theta}}_2\mathbf{I}\dot{\mathbf{u}} + \dot{\widehat{\boldsymbol{\theta}}}_2\mathbf{I}\mathbf{u} - \dot{\boldsymbol{\alpha}}_2\\ &= \widehat{\boldsymbol{\theta}}_2\mathbf{I}\mathbf{T}^{-1}\mathbf{u}_c - \widehat{\boldsymbol{\theta}}_2\mathbf{I}\mathbf{T}^{-1}\mathbf{u} + \dot{\widehat{\boldsymbol{\theta}}}_2\mathbf{I}\mathbf{u} - \dot{\boldsymbol{\alpha}}_2\end{aligned} \quad (13)$$

The positive definite (Assumption 1.1) control Lyapunov function (CLF) for the entire system (1)-(4) is considered as the weighted sum of output errors $\mathbf{z}_i$ augmented by $\mathbf{V}_{phi}$ which depend on parameter estimate errors and will be formulated later.

$$\mathbf{V}_a = \tfrac{1}{2}\mathbf{z}_1^T\mathbf{z}_1 + \tfrac{1}{2}\mathbf{z}_2^T\mathbf{M}\mathbf{z}_2 + \tfrac{1}{2}\mathbf{z}_3^T\mathbf{z}_3 + \mathbf{V}_{phi} \quad (14)$$

Evaluating the time derivative of CLF along the state trajectories (19), (12), (13), and assuming $-\mathbf{z}_1^T r\mathbf{S}\mathbf{z}_1 = 0$ yields:

$$\begin{aligned}\dot{\mathbf{V}}_a &= \mathbf{z}_1^T\dot{\mathbf{z}}_1 + \mathbf{z}_2^T\mathbf{M}\dot{\mathbf{z}}_2 + \mathbf{z}_3^T\dot{\mathbf{z}}_3 + \dot{\mathbf{V}}_{phi}\\ &= \mathbf{z}_1^T[\boldsymbol{\alpha}_1 - \mathbf{J}(\boldsymbol{\eta})^T\dot{\boldsymbol{\eta}}_d] + \mathbf{z}_2^T\left[\mathbf{z}_1 + \boldsymbol{\alpha}_2 + \boldsymbol{\varphi}_1^T(\boldsymbol{\eta},\mathbf{v})\widehat{\boldsymbol{\theta}}_1 - \mathbf{M}\dot{\boldsymbol{\alpha}}_1\right]\\ &+\mathbf{z}_3^T\left[\mathbf{z}_2 + \widehat{\boldsymbol{\theta}}_2\mathbf{I}\mathbf{T}^{-1}\mathbf{u}_c - \widehat{\boldsymbol{\theta}}_2\mathbf{I}\mathbf{T}^{-1}\mathbf{u} + \dot{\widehat{\boldsymbol{\theta}}}_2\mathbf{I}\mathbf{u} - \dot{\boldsymbol{\alpha}}_2\right]\\ &+\mathbf{z}_2^T(\widetilde{\boldsymbol{\theta}}_2\mathbf{I}\mathbf{u} + \boldsymbol{\varphi}_1^T(\boldsymbol{\eta},\mathbf{v})\widetilde{\boldsymbol{\theta}}_1) + \dot{\mathbf{V}}_{phi}\end{aligned} \quad (15)$$

Now, according to LaSalle's invariance principle, the controls α_1, α_2, $\mathbf{u}_c$, and the estimates $\widehat{\boldsymbol{\theta}}_1, \widehat{\boldsymbol{\theta}}_2$ are chosen to make (15) negative semidefinite, that is

$$\dot{\mathbf{V}}_a = -\mathbf{z}_1^T\mathbf{G}_1\mathbf{z}_1 - \mathbf{z}_2^T\mathbf{G}_2\mathbf{z}_2 - \mathbf{z}_3^T\mathbf{G}_3\mathbf{z}_3 \leq 0 \quad (16)$$

with the control gain matrices $\mathbf{G}_i \in \mathrm{R}^{3\times3}$, $i = \{1,2,3\}$, diagonal and positive definite. According to this, the CLF (15) is to be divided into components which depend and do not depend on the estimate errors.

The process is carried out in several steps. In the first step, the vector of stabilizing functions $\boldsymbol{\alpha}_1$ is chosen independently from uncertainties to make the first bracket term of (15) equal to $-\mathbf{G}_1\mathbf{z}_1$:

$$\boldsymbol{\alpha}_1 = -\mathbf{G}_1\mathbf{z}_1 + \mathbf{J}(\boldsymbol{\eta})^T\dot{\boldsymbol{\eta}}_d \tag{17}$$

Then, the controls $\boldsymbol{\alpha}_2$, $\mathbf{u}_c$ can be implemented, due to the fact that the vectors $\boldsymbol{\theta}_1$ and $\boldsymbol{\theta}_2$ are unknown. Following this, the vector of stabilizing functions $\boldsymbol{\alpha}_2$ is chosen as:

$$\boldsymbol{\alpha_2} = -\mathbf{G}_2\mathbf{z}_2 - \mathbf{z}_1 + \mathbf{M}\dot{\boldsymbol{\alpha}}_1 - \boldsymbol{\varphi}_1^T(\boldsymbol{\eta},\mathbf{v})\widehat{\boldsymbol{\theta}}_1 \tag{18}$$

where

$$\dot{\boldsymbol{\alpha}}_1 = -\mathbf{G}_1\dot{\mathbf{z}}_1 - r\mathbf{S}\mathbf{J}(\boldsymbol{\eta})^T\dot{\boldsymbol{\eta}}_d + \mathbf{J}(\boldsymbol{\eta})^T\ddot{\boldsymbol{\eta}}_d \tag{19}$$

Let us analytically calculate the first time derivative of $\boldsymbol{\alpha}_2$:

$$\begin{aligned}\dot{\boldsymbol{\alpha}}_2 = &-\mathbf{G}_2\dot{\mathbf{z}}_2 - \dot{\mathbf{z}}_1 + \mathbf{M}\ddot{\boldsymbol{\alpha}}_1\\ &-\boldsymbol{\varphi}_1^T(\boldsymbol{\eta},\mathbf{v})\dot{\widehat{\boldsymbol{\theta}}}_1 - \dot{\boldsymbol{\varphi}}_1^T(\boldsymbol{\eta},\mathbf{v})\widehat{\boldsymbol{\theta}}_1\end{aligned} \tag{20}$$

Note that the last component in (20) can be rewritten into (21), based on **Assumption 1.3**, and assuming that current velocities are constant or slowly varying, so $\dot{\mathbf{v}}_c = \mathbf{0}$.

$$\begin{aligned}\dot{\boldsymbol{\varphi}}_1^T(\boldsymbol{\eta},\mathbf{v})\widehat{\boldsymbol{\theta}}_1 = &-\widehat{\mathbf{D}}\dot{\mathbf{v}} - r\mathbf{S}\mathbf{J}^T\hat{\mathbf{b}}\\ = &-\widehat{\mathbf{D}}\mathbf{M}^{-1}(\boldsymbol{\theta}_2\mathbf{I}\mathbf{u} + \boldsymbol{\varphi}_1^T(\boldsymbol{\eta},\mathbf{v})\boldsymbol{\theta}_1) - r\mathbf{S}\mathbf{J}^T\hat{\mathbf{b}}\end{aligned} \tag{21}$$

where

$$\widehat{\mathbf{D}} = -\begin{bmatrix}\widehat{\boldsymbol{\theta}}_1(1) & 0 & 0\\ 0 & \widehat{\boldsymbol{\theta}}_1(2) & \widehat{\boldsymbol{\theta}}_1(3)\\ 0 & \widehat{\boldsymbol{\theta}}_1(4) & \widehat{\boldsymbol{\theta}}_1(5)\end{bmatrix},\ \hat{\mathbf{b}} = [\widehat{\boldsymbol{\theta}}_1(6), \widehat{\boldsymbol{\theta}}_1(7), \widehat{\boldsymbol{\theta}}_1(8)]^T$$

are the estimates of $\mathbf{D}$ and $\mathbf{b}$. Substituting (21) and (10) into (20), we get (22)

$$\begin{aligned}\dot{\boldsymbol{\alpha}}_2 = &-\mathbf{G}_2[\mathbf{M}^{-1}(\boldsymbol{\theta}_2\mathbf{I}\mathbf{u} + \boldsymbol{\varphi}_1^T(\boldsymbol{\eta},\mathbf{v})\boldsymbol{\theta}_1 - \mathbf{M}\dot{\boldsymbol{\alpha}}_1)] - \dot{\mathbf{z}}_1 + \mathbf{M}\ddot{\boldsymbol{\alpha}}_1\\ &+ \widehat{\mathbf{D}}\mathbf{M}^{-1}(\boldsymbol{\theta}_2\mathbf{I}\mathbf{u} + \boldsymbol{\varphi}_1^T(\boldsymbol{\eta},\mathbf{v})\boldsymbol{\theta}_1) + r\mathbf{S}\mathbf{J}^T\hat{\mathbf{b}} - \boldsymbol{\varphi}_1^T(\boldsymbol{\eta},\mathbf{v})\dot{\widehat{\boldsymbol{\theta}}}_1\end{aligned} \tag{22}$$

Furthermore, using the principle certain equivalence yields

$$\begin{aligned}&\boldsymbol{\theta}_2\mathbf{I}\mathbf{u} + \boldsymbol{\varphi}_1^T(\boldsymbol{\eta},\mathbf{v})\boldsymbol{\theta}_1\\ &= \widehat{\boldsymbol{\theta}}_2\mathbf{I}\mathbf{u} + \boldsymbol{\varphi}_1^T(\boldsymbol{\eta},\mathbf{v})\widehat{\boldsymbol{\theta}}_1 + \widetilde{\boldsymbol{\theta}}_2\mathbf{I}\mathbf{u} + \boldsymbol{\varphi}_1^T(\boldsymbol{\eta},\mathbf{v})\widetilde{\boldsymbol{\theta}}_1\end{aligned} \tag{23}$$

Substituting (23) into (22) yields

$$\dot{\boldsymbol{\alpha}}_2 = \dot{\widehat{\boldsymbol{\alpha}}}_2 - (\mathbf{G}_2 - \widehat{\mathbf{D}})\mathbf{M}^{-1}(\widetilde{\boldsymbol{\theta}}_2\mathbf{I}\mathbf{u} + \boldsymbol{\varphi}_1^T(\boldsymbol{\eta},\mathbf{v})\widetilde{\boldsymbol{\theta}}_1) \tag{24}$$

where $\dot{\widehat{\boldsymbol{\alpha}}}_2$ does not depend on estimate errors.

$$\begin{aligned}\dot{\widehat{\boldsymbol{\alpha}}}_2 = &-\mathbf{G}_2\left[\mathbf{M}^{-1}\left(\widehat{\boldsymbol{\theta}}_2\mathbf{I}\mathbf{u} + \boldsymbol{\varphi}_1^T(\boldsymbol{\eta},\mathbf{v})\widehat{\boldsymbol{\theta}}_1\right) - \dot{\boldsymbol{\alpha}}_1\right] - \dot{\mathbf{z}}_1 + \mathbf{M}\ddot{\boldsymbol{\alpha}}_1\\ &+ \widehat{\mathbf{D}}\mathbf{M}^{-1}\left(\widehat{\boldsymbol{\theta}}_2\mathbf{I}\mathbf{u} + \boldsymbol{\varphi}_1^T(\boldsymbol{\eta},\mathbf{v})\widehat{\boldsymbol{\theta}}_1\right) + r\mathbf{S}\mathbf{J}^T\hat{\mathbf{b}} - \boldsymbol{\varphi}_1^T(\boldsymbol{\eta},\mathbf{v})\dot{\widehat{\boldsymbol{\theta}}}_1\end{aligned}$$

After replacing $\boldsymbol{\alpha_1}, \boldsymbol{\alpha_2}$ and $\dot{\boldsymbol{\alpha}}_2$ into (15) by (17), (18) and (24), respectively, the time derivative of CLF satisfies

$$\begin{aligned}\dot{\mathbf{V}}_a = &-\mathbf{z}_1^T\mathbf{G}_1\mathbf{z}_1 - \mathbf{z}_2^T\mathbf{G}_2\mathbf{z}_2\\ &+\mathbf{z}_3^T\left[\mathbf{z}_2 + \widehat{\boldsymbol{\theta}}_2\mathbf{I}\mathbf{T}^{-1}\mathbf{u}_c - \widehat{\boldsymbol{\theta}}_2\mathbf{I}\mathbf{T}^{-1}\mathbf{u} + \dot{\widehat{\boldsymbol{\theta}}}_2\mathbf{I}\mathbf{u} - \dot{\widehat{\boldsymbol{\alpha}}}_2\right]\\ &+\mathbf{z}_3^T\left[(\mathbf{G}_2 - \widehat{\mathbf{D}})\mathbf{M}^{-1}(\widetilde{\boldsymbol{\theta}}_2\mathbf{I}\mathbf{u} + \boldsymbol{\varphi}_1^T(\boldsymbol{\eta},\mathbf{v})\widetilde{\boldsymbol{\theta}}_1)\right]\\ &+\mathbf{z}_2^T\left(\widetilde{\boldsymbol{\theta}}_2\mathbf{I}\mathbf{u} + \boldsymbol{\varphi}_1^T(\boldsymbol{\eta},\mathbf{v})\widetilde{\boldsymbol{\theta}}_1\right) + \dot{\mathbf{V}}_{phi}\end{aligned} \tag{25}$$

Note, that matrix $\widetilde{\boldsymbol{\theta}}_2$ has a dimension 3 by r and cannot be used directly in the augmented component $\dot{\mathbf{V}}_{phi}$ of CLF according to the standard backstepping method. To eliminate $\widetilde{\boldsymbol{\theta}}_2$ from (25) we need to rewrite the expression $\widetilde{\boldsymbol{\theta}}_2\mathbf{I}\mathbf{u}$ to the regression form (26).

$$\widetilde{\boldsymbol{\theta}}_2\mathbf{I}\mathbf{u} = \boldsymbol{\varphi}_3^T(\mathbf{u})\widetilde{\boldsymbol{\theta}}_3 \tag{26}$$

with the regression matrix $\boldsymbol{\varphi}_3^T(\mathbf{u}) = \begin{bmatrix}\mathbf{I}\mathbf{u}^T & \mathbf{0}_{1\times\mathrm{r}} & \mathbf{0}_{1\times\mathrm{r}}\\ \mathbf{0}_{1\times\mathrm{r}} & \mathbf{I}\mathbf{u}^T & \mathbf{0}_{1\times\mathrm{r}}\\ \mathbf{0}_{1\times\mathrm{r}} & \mathbf{0}_{1\times\mathrm{r}} & \mathbf{I}\mathbf{u}^T\end{bmatrix} \in R^{3\times3\mathrm{r}}$ and the auxiliary vector $\widetilde{\boldsymbol{\theta}}_3 \in \mathrm{R}^{3\mathrm{r}\times1}$ containing all parameter estimation errors included in matrix $\widetilde{\boldsymbol{\theta}}_2$.

Representing $\widetilde{\boldsymbol{\theta}}_2 = \begin{bmatrix}\widetilde{\boldsymbol{\theta}}_{21}\\ \widetilde{\boldsymbol{\theta}}_{22}\\ \widetilde{\boldsymbol{\theta}}_{23}\end{bmatrix} \in \mathrm{R}^{3\times\mathrm{r}}$ as the blocked matrix with rows of $\widetilde{\boldsymbol{\theta}}_{2i} \in \mathrm{R}^{1\times\mathrm{r}}$, $i = 1,2,3$, leads to $\widetilde{\boldsymbol{\theta}}_3 = [\widetilde{\boldsymbol{\theta}}_{21}|\widetilde{\boldsymbol{\theta}}_{22}|\widetilde{\boldsymbol{\theta}}_{23}]^T \in \mathrm{R}^{3\mathrm{r}\times1}$. Then, after using $\dot{\widetilde{\boldsymbol{\theta}}}_3 = -\dot{\widehat{\boldsymbol{\theta}}}_3$, the relation between estimates can be set as:

$$\dot{\widehat{\boldsymbol{\theta}}}_3 = [\dot{\widehat{\boldsymbol{\theta}}}_{21}|\dot{\widehat{\boldsymbol{\theta}}}_{22}|\dot{\widehat{\boldsymbol{\theta}}}_{23}]^T \in \mathrm{R}^{3\mathrm{r}\times1} \tag{27}$$

Choosing $\mathbf{V}_{phi} = \widetilde{\boldsymbol{\theta}}_1^T{\boldsymbol{\Gamma}_1}^{-1}\widetilde{\boldsymbol{\theta}}_1 + \widetilde{\boldsymbol{\theta}}_3^T{\boldsymbol{\Gamma}_3}^{-1}\widetilde{\boldsymbol{\theta}}_3$ as the weighted sum of estimate errors $\widetilde{\boldsymbol{\theta}}_1$ and $\widetilde{\boldsymbol{\theta}}_3$, where $\boldsymbol{\Gamma}_1 \in \mathrm{R}^{8\times8}$ and $\boldsymbol{\Gamma}_3 \in \mathrm{R}^{3\mathrm{r}\times3\mathrm{r}}$ are diagonal and positive adaptive gain matrices and approximately assuming that $\dot{\widetilde{\boldsymbol{\theta}}}_i = -\dot{\widehat{\boldsymbol{\theta}}}_i$ yields

$$\dot{\mathbf{V}}_{phi} = -\widetilde{\boldsymbol{\theta}}_1^T{\boldsymbol{\Gamma}_1}^{-1}\dot{\widehat{\boldsymbol{\theta}}}_1 - \widetilde{\boldsymbol{\theta}}_3^T{\boldsymbol{\Gamma}_3}^{-1}\dot{\widehat{\boldsymbol{\theta}}}_3 \tag{28}$$

Choosing the control law $\mathbf{u}_c$ as in (25) satisfies

$$\widehat{\boldsymbol{\theta}}_2\mathbf{I}\mathbf{T}^{-1}\mathbf{u}_c = -\mathbf{G}_3\mathbf{z}_3 - \mathbf{z}_2 + \widehat{\boldsymbol{\theta}}_2\mathbf{I}\mathbf{T}^{-1}\mathbf{u} - \dot{\widehat{\boldsymbol{\theta}}}_2\mathbf{I}\mathbf{u} + \dot{\widehat{\boldsymbol{\alpha}}}_2 \tag{29}$$

The derivative of the augmented Lyapunov function is finally equal to

$$\begin{aligned}\dot{\mathbf{V}}_a = &-\mathbf{z}_1^T\mathbf{G}_1\mathbf{z}_1 - \mathbf{z}_2^T\mathbf{G}_2\mathbf{z}_2 - \mathbf{z}_3^T\mathbf{G}_3\mathbf{z}_3\\ &+\widetilde{\boldsymbol{\theta}}_1^T[\boldsymbol{\varphi}_1(\boldsymbol{\eta},\mathbf{v})(\mathbf{M}^{-T}\left(\mathbf{G}_2 - \widehat{\mathbf{D}}\right)^T\mathbf{z}_3 + \mathbf{z}_2) - {\boldsymbol{\Gamma}_1}^{-1}\dot{\widehat{\boldsymbol{\theta}}}_1]\\ &+\widetilde{\boldsymbol{\theta}}_3^T[\boldsymbol{\varphi}_3(\mathbf{u})(\mathbf{M}^{-T}\left(\mathbf{G}_2 - \widehat{\mathbf{D}}\right)^T\mathbf{z}_3 + \mathbf{z}_2) - {\boldsymbol{\Gamma}_3}^{-1}\dot{\widehat{\boldsymbol{\theta}}}_3]\end{aligned} \tag{30}$$

After using (30), the adaptive laws chosen to enforce the closed-loop stability take the form

$$\dot{\widehat{\boldsymbol{\theta}}}_1 = \boldsymbol{\Gamma}_1\boldsymbol{\varphi}_1(\boldsymbol{\eta},\mathbf{v})[\mathbf{M}^{-T}\left(\mathbf{G}_2 - \widehat{\mathbf{D}}\right)^T\mathbf{z}_3 + \mathbf{z}_2] \tag{31}$$

$$\dot{\widehat{\boldsymbol{\theta}}}_3 = \boldsymbol{\Gamma}_3\boldsymbol{\varphi}_3(\mathbf{u})[\mathbf{M}^{-T}\left(\mathbf{G}_2 - \widehat{\mathbf{D}}\right)^T\mathbf{z}_3 + \mathbf{z}_2] \tag{32}$$

To obtain the estimate of vector $\boldsymbol{\theta_2}$, first the vector $\boldsymbol{\theta_3}$ is estimated in accordance with the adaptation rule (32), then taking the action reverse to (26) the estimate $\widehat{\boldsymbol{\theta}}_2$ can be calculated dynamically from (27) that describes relation between $\widehat{\boldsymbol{\theta}}_2$ and $\widehat{\boldsymbol{\theta}}_3$.

In fact, due to (29)-(31), the time derivative of CLF becomes negative semidefinite

$$\dot{\mathbf{V}}_a = -\mathbf{z}_1^T\mathbf{G}_1\mathbf{z}_1 - \mathbf{z}_2^T\mathbf{G}_2\mathbf{z}_2 - \mathbf{z}_3^T\mathbf{G}_3\mathbf{z}_3 \leq 0 \qquad (33)$$

3.2 Control Allocation

The adaptive backstepping procedure (29) gives the adaptive virtual control commands $\boldsymbol{\tau}_c \in \mathrm{R}^{3\times1}$

$$\boldsymbol{\tau}_c = -\mathbf{G}_3\mathbf{z}_3 - \mathbf{z}_2 + \widehat{\boldsymbol{\theta}}_2\mathbf{I}\mathbf{T}^{-1}\mathbf{u} - \dot{\widehat{\boldsymbol{\theta}}}_2\mathbf{I}\mathbf{u} + \dot{\widehat{\boldsymbol{\alpha}}}_2 \qquad (34)$$

for the control allocation unit, which distributes the input $\boldsymbol{\tau}_c$ among the thrusters $\mathbf{u}_c \in \mathrm{R}^{\mathrm{r}\times1}$, and incorporates the lower and upper actuator position and rate (35) while minimizing power consumption by actuators.

$$\begin{aligned} \dot{\mathbf{u}}_{c_{min}} \leq \dot{\mathbf{u}}_c \leq \dot{\mathbf{u}}_{c_{max}} \\ \mathbf{u}_{c_{min}} \leq \mathbf{u}_c \leq \mathbf{u}_{c_{max}} \end{aligned} \qquad (35)$$

The equation to be solved for $\mathbf{u}_c$ takes the form (36)

$$\widehat{\boldsymbol{\theta}}_2\mathbf{I}\mathbf{T}^{-1}\mathbf{u}_c = \boldsymbol{\tau}_c \qquad (36)$$

According to **Assumption 1.4** and neglecting actuator constraints, the control allocation rule takes the form

$$\mathbf{u}_c = \mathbf{T}\mathbf{I}\widehat{\boldsymbol{\theta}}_2^{+}\boldsymbol{\tau}_c \qquad (37)$$

where $\widehat{\boldsymbol{\theta}}_2^{+}$ denotes the Moore - Penrose pseudo - inverse matrix.

For a ship with a redundant set of actuators, the problem of control allocation can be formulated as a sequential quadratic programming:

$$\boldsymbol{\Omega}: \min_{\mathbf{u}_{c_{min}} \leq \mathbf{u}_c \leq \mathbf{u}_{c_{max}}} \left\| \widehat{\boldsymbol{\theta}}_2\mathbf{I}\mathbf{T}^{-1}\mathbf{u}_c - \boldsymbol{\tau}_c \right\|_2 \qquad (38)$$

$$\mathbf{u}_c: \min_{\mathbf{u}_c \in \boldsymbol{\Omega}} \|\mathbf{W}\mathbf{u}_c\|_2 \qquad (39)$$

In the first instance, the set $\boldsymbol{\Omega}$ of feasible control inputs $\mathbf{u}_c \in \mathbf{R}^{\mathrm{r}\times1}$ which minimizes the equation (38) is chosen with respect to (36). In the second instance the control input $\mathbf{u}_c$ is chosen from $\boldsymbol{\Omega}$ that minimizes the cost function (39), weighted by W$\in \mathbf{R}^{\mathrm{r}\times\mathrm{r}}$.

4. NUMERICAL SIMULATIONS

Simulation tests have been performed for a supply vessel with the mass m = 4591[t] and the length L = 76.2 m. The parameters of the matrix system (1)-(4) were defined in accordance with the Bis-scaled system (Fossen et al. 1996) as:

D"= [0.0358 0 0; 0 0.1183 -0.0124; 0 -0.0041 0.0308];

M"= **[**1.1274 0 0; 0 1.8902 -0.0744; 0 -0.0744 0.1278**]**;

B"=[1 1 0 0 0 0 ;0 0 1 1 1 1; 0.0472 -0.0472 -0.4108 -0.3858 0.4554 0.33373]; **K"**=diag([9.3 9.3 2.0 2.0 2.8 2.6])10^{-3};

T"=5.0$\sqrt{g/L}\mathbf{I}_{6x6}$, where g = 9.81 m/s^2.

The actuator time constants were chosen equal to 5s for all thrusters and propellers. Also, the constraints of the dimensional model were considered: $|u| \leq \frac{4\mathrm{m}}{\mathrm{s}}, |v| \leq 1\frac{\mathrm{m}}{\mathrm{s}}, |r| \leq 1\frac{\mathrm{deg}}{\mathrm{s}}$. The supply vessel is equipped with two main propellers (port and starboard), two aft and one bow tunnel thrusters, and one rotatable bow azimuth thruster. The control input vector consists of six elements, respectively $\mathbf{u}_c = [u_1, u_2, u_3, u_4, u_5, u_6]^T$ where the thruster inputs are scaled such that $|u_i^{"}| \leq 1, i \in \{1, \ldots, 6\}$. The simulations were performed in Matlab/Simulink with the dimensionless sampling time $h^{"} = 0.1$, corresponding to $h = 0.2788$. The vessel is exposed to slowly varying environmental disturbances, modelled by the 1-order Markov process. The initial values of the estimated parameters for the controller settings were equal to $\widehat{\boldsymbol{\theta}}_1(0) = \mathbf{0}$ and $\widehat{\boldsymbol{\theta}}_3(0) = 0.8\boldsymbol{\theta}_3(0)$. The remaining parameters of the controller are $\mathbf{G_1} = 0.001\mathbf{I}$, $\mathbf{G_2} = \mathbf{G_3} = 0.03\mathbf{I}$, $\boldsymbol{\Gamma}_1 = 0.01\mathbf{I}$, $\boldsymbol{\Gamma}_3 = \mathbf{I}$. The simulation results are depicted in Fig. 1-8. The figures present the control performance of the adaptive backstepping DP control law with control allocation in the presence of partial loss of actuator effectiveness (Fig. 1-4) and total loss of actuator effectiveness (Fig. 5-8), both cases compared to the fault-free case. It was assumed during the partial loss of actuator effectiveness faults that all actuators work, so $\mathbf{I} = diag(1,1,1,1,1,1)$, but the control effectiveness matrix changed. For the total loss of actuator effectiveness faults, it was assumed that some actuators failed, what was modelled by changing of matrix **I**. The tests analysed in Fig. 1-4 refer to: Test 1 - fault-free case; Test 2 - 80% loss of aft tunnel thrust II, so k_4=0.2k_4 after 278.8 s; Test 3 - 80% loss of bow azimuth thruster effectiveness after 278.8 s, k_6=0.2k_6.

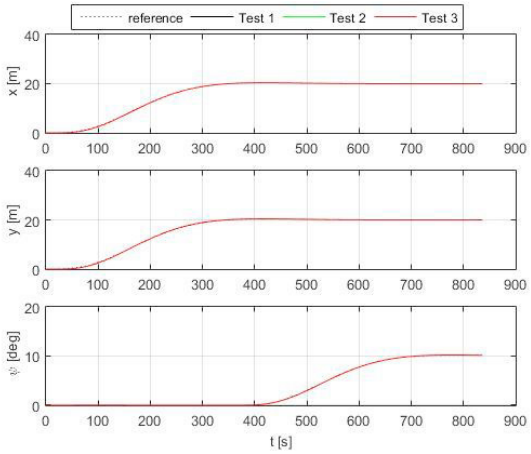

Fig. 1. Actual ($\boldsymbol{\eta}$) and desired ($\boldsymbol{\eta}_\mathrm{d}$) ship position and heading - partial loss of actuator effectiveness faults.

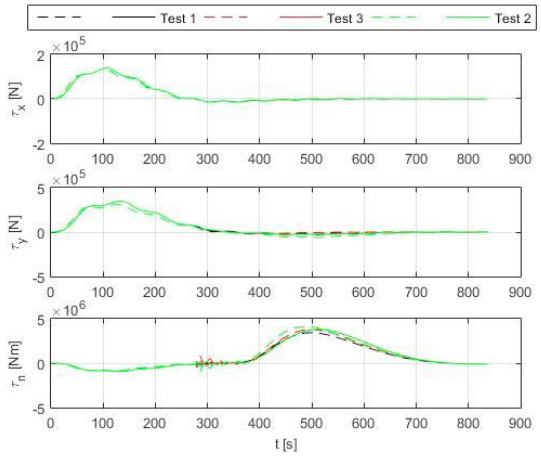

Fig. 2. Command control forces ($\hat{\boldsymbol{\tau}}_c$ – dotted line) and actual control forces ($\boldsymbol{\tau}$ – solid line) generated by actuators - partial loss of actuator effectiveness faults.

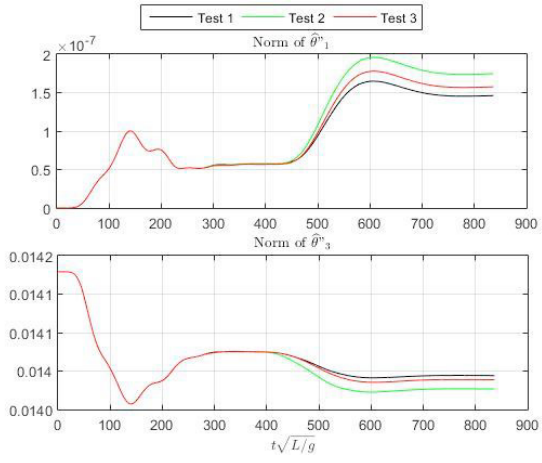

Fig. 3. Bis-scaled 2-norms ($\|\widehat{\boldsymbol{\theta}}_1\|$, $\|\widehat{\boldsymbol{\theta}}_3\|$) of parameter estimates of $\boldsymbol{\theta}_1$ and $\boldsymbol{\theta}_3$ - partial loss of actuator effectiveness faults.

The tests analysed in Fig. 5-8 refer to: Test 1 - fault-free case; Test 2 - aft tunnel thruster II failure after 278.8 s, so $\mathbf{I} = diag(1,1,0,1,1,1)$; Test 3 - bow tunnel thruster failure after the same time, so $\mathbf{I} = diag(1,1,1,1,0,1)$. It can be clearly observed in Fig. 1 and Fig. 5 that the proposed algorithm asymptotically regulates the position and heading to their desired values in the presence of unknown model parameters, disturbances uncertainties, and thrust faults. The control errors tend to zero. The command control forces calculated from the adaptive control allocation law are compared in Fig.2 and Fig.6 with actual forces generated by ship actuators. The Bis-scaled command and real actuator values calculated from CGI control allocation algorithm are shown in Fig. 4 and Fig. 8. Fig. 3 and Fig. 7 present the norms of estimates $\|\widehat{\boldsymbol{\theta}}_1\|$, $\|\widehat{\boldsymbol{\theta}}_3\|$ of controller parameters which change relatively slowly. It can be clearly observed that the norms of estimates change within a limited range due to the change of ship position and heading, or due to environmental disturbances and/or actuator failures.

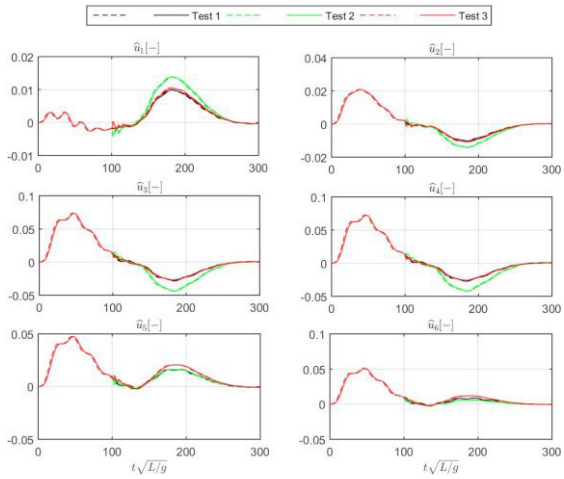

Fig. 4. Bis-scaled command actuator signal ($\hat{\mathbf{u}}_c$ - dotted line) and real actuator signal ($\mathbf{u}$ - solid line) - partial loss of actuator effectiveness faults.

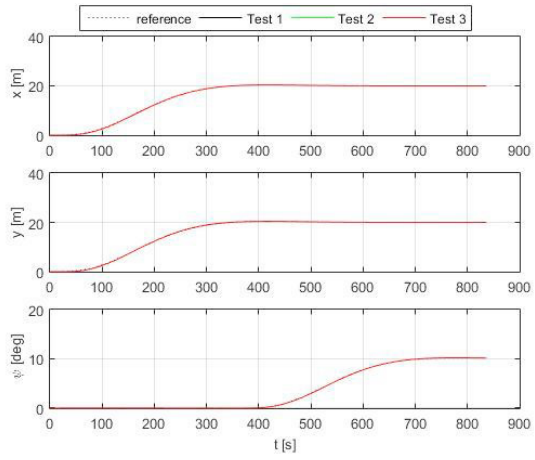

Fig. 5. Actual ($\boldsymbol{\eta}$) and desired ($\boldsymbol{\eta}_d$) ship position and heading - total loss of actuator effectiveness faults.

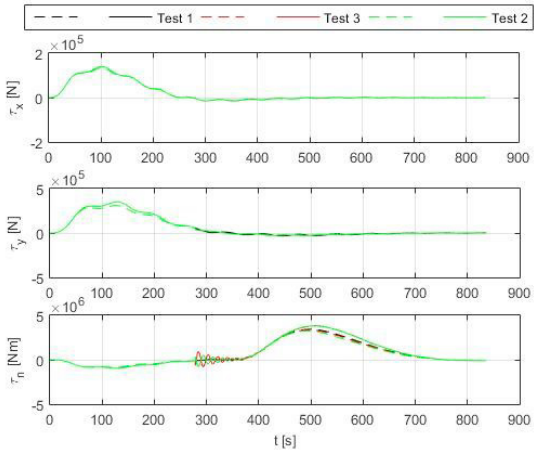

Fig. 6. Command control forces ($\hat{\boldsymbol{\tau}}_c$ – dotted line) and actual control forces ($\boldsymbol{\tau}$ – solid line) generated by actuators - total loss of actuator effectiveness faults.

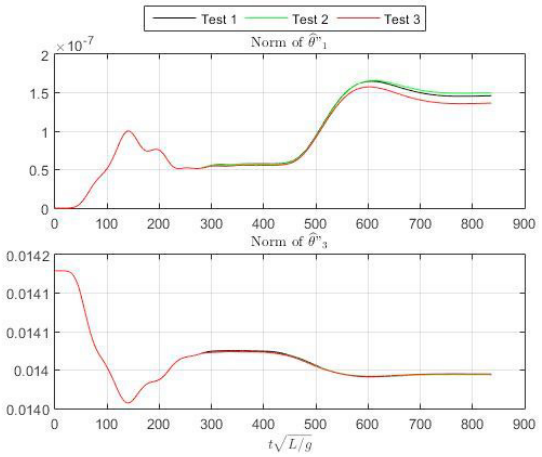

Fig. 7. Bis-scaled 2-norms ($\|\widehat{\boldsymbol{\theta}}_1\|$, $\|\widehat{\boldsymbol{\theta}}_3\|$) of parameter estimates of $\boldsymbol{\theta}_1$ and $\boldsymbol{\theta}_3$ - total loss of actuator effectiveness faults.

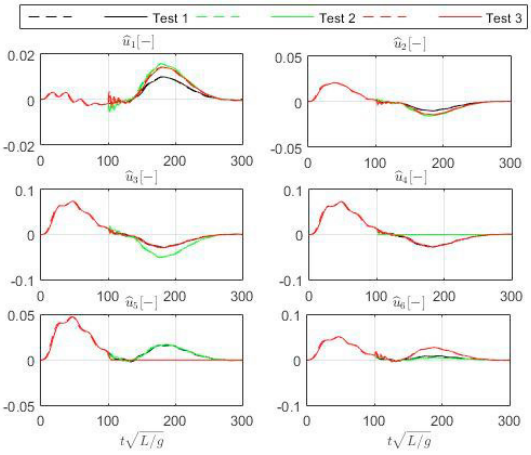

Fig. 8. Bis-scaled command actuator signals ($\widehat{\mathbf{u}}_\mathbf{c}$ - dotted line) and real actuator signals ($\mathbf{u}$ - solid line) - total loss of actuator effectiveness faults.

The estimated parameters are almost bounded, which demonstrates that the proposed DP adaptive control law is effective and has satisfactory performance also in case of unknown actuator forces.

5. CONCLUSIONS

The results show that the proposed adaptive control allocation law based backstepping method can maintain the ship position and heading at the desired values with satisfactory performance, at the same time guaranteeing that all signals in the closed-loop DP control system are uniformly ultimately bounded (UUB). The proposed design procedure is general, and can be applied to other marine vessels which operate at low speed, including aircrafts or mobile robots represented by similar state-space model.

REFERENCES

Benetazzo, F., Ippoliti, G., Longhi, S. and Raspa, P. (2015). Advanced control for fault-tolerant dynamic positioning of an offshore supply vessel. *Ocean Engineering* (106), 472-484.

Fossen, T. (2011). Handbook of Marine Craft Hydrodynamics and Motion Control. John Wiley and Sons Ltd, Chichester.

Krsti´c, M., Kanellakopoulos, I. and Kokotovi´c, P. (1995). *Nonlinear and Adaptive Control Design*. Wiley, New York, NY, USA.

Johansen, T. and Fossen, T. (2013). Control allocation a survey. *Automatica* 49(5), 1087–1103.

Lin, Y., Du, J., (2016). Fault-Tolerant Control for Dynamic Positioning of Ships Based on an Iterative Learning Observer. *Proceedings of the 35th Chinese Control* Conference, pp. 1116-1122.

Lindegaard, K. and Fossen, T. (2003). Fuel-efficient rudder and propeller control allocation for marine craft: Experiments with a model ship, IEEE Trans. Control Syst. Technol. 11: 850–862.

Loria, A., Fossen, T. and Panteley, E. (2000). A separation principle for dynamic positioning of ships: Theoretical and experimental results. *IEEE Transactions on Control Systems Technology* 8(2), 332–343.

Oppenheimer, M., Doman, D. and Bolender, M. (2006). Control allocation for over-actuated systems, Proceedings of 14th Mediterranean Conference on Control and Automation, pp. 1–6.

Oppenheimer, M., Doman, D., Yurkovich, S., Serrani, A. and Luo, A. (2004). Model predictive dynamic control allocation with actuator dynamic, Proceedings of 2004 American Control Conference, pp. 1695–1700.

Sorensen, A. (2011). A survey of dynamic positioning control systems, Annual Reviews in Control 35(1): 123–136.

Su, Y., Zheng, Ch. and Mercorelli, P. (2017). Nonlinear PD Fault-Tolerant Control for Dynamic Positioning of Ships with Actuator Constraints. *IEEE/ASME Transactions on Mechatronics*, 22(3), 1132-1142.

Tjønnås, J. and Johansen, T. A. (2005). Adaptive optimizing nonlinear control allocation. *Proceedings of the 16th IFAC World Congress, Prague*, 38 (1), 1160-1165.

Tjønnås, J. and Johansen, T. A. (2007). Optimizing adaptive control allocation with actuator dynamics. *Proceedings of 46th IEEE Conference on Decision and Control*, pp. 3780-3785.

Zhang, J.X. and Yang G.H. (2017). Robust Adaptive Fault-Tolerant Control for a Class of Unknown Nonlinear Systems. *IEEE Transactions on Industrial Electronics*, 64(1), 585–594.